Organic & Biomolecular Chemistry

Accepted Manuscript

ROYAL SOCIETY OF CHEMISTRY

www.rsc.org/obc

Journal Name
Organic & Biomolecular Chemistry
Dynamic Article Links ►

Cite this: DOI: 10.1039/c0xx00000x

www.rsc.org/xxxxxx

ARTICLE TYPE

Synthesis and Biological Evaluation of Novel Pyrano[3,2-*c*]carbazole Derivatives as Anti-tumor Agents inducing apoptosis via tubulin polymerization inhibition

Pannala Padmaja,*[a] Garikapati Koteswara Rao,[b] Adisherla Indrasena,[a] Basireddy V. Subba Reddy,[b] Nibedita Patel,[b] Anver Basha Shaik,[b] Narayana Reddy,[c] Pramod K. Dubey,[a] Manika Pal Bhadra*[b]

Received (in XXX, XXX) Xth XXXXXXXXX 20XX, Accepted Xth XXXXXXXXX 20XX
DOI: 10.1039/b000000x

A series of novel pyrano[3,2-*c*]carbazole derivatives have been synthesized in a simple one-pot, three component reaction of aromatic aldehydes, malononitrile/ethylcyanoacetate and 4-hydroxycarbazoles catalyzed by triethylamine. The antiproliferative activity of the derivatives were investigated on various cancer cell lines such as MDA-MB-231, K562, A549 and HeLa. Congeners **9a**, **9c**, **9g** and **9i** among **9a-p** showed profound antiproliferative activity with an IC_{50} values ranging from 0.43-8.05 μM and induced apoptosis significantly by inhibiting tubulin polymerization. Cell-based biological assays demonstrated that treatment of cell lines with compounds **9a**, **9c**, **9g** and **9i** result in G2/M phase arrest of cell cycle. Moreover the derivatives significantly disrupted microtubule network, produced an elevation of cyclinB1 protein and induced apoptosis by increasing the caspase-3 levels. In particular, **9i** strongly inhibited tubulin assembly compared to the positive control CA-4. Molecular docking studies demonstrated that all the lead compounds selectively occupy the colchicine binding site of the tubulin polymer.

Introduction

Carbazoles display a wide range of biological activities, making them attractive compounds to synthetic and medicinal chemists.[1-6] Many carbazole derivatives are used as organic materials, due to their photorefractive, photoconductive, whole transporting and light-emitting properties.[7] Several carbazoles are known for their potent antitumor, antibacterial, anti-tuberculosis, anti-inflammatory, psychotropic and anti-histaminic properties.[8-11] Among them pyranocarbazole alkaloids such as grinimbine, mupamine, mahanimbine, murrayanol and mahanine, which have been isolated from plants of the Rutaceae family,[12] possess osquitocidal, antimicrobial, anti-inflammatory and antioxidant activities.[13,14] Grinimbine **1** (Fig.1) and isomahanine **3** have been reported to possess significant cytotoxicity against lung cancer (NCI-522),[15-17] whereas koenimbine showed rapid scavenging activities against the 1,1-diphenyl- 2-picrylhydrazyl (DPPH) radical.[18] The broad range of useful biological activities exhibited by pyranocarbazole alkaloids prompted several research groups to develop synthetic strategies such as domino aldol-type/6π-electrocyclization,[19] palladium-catalyzed intramolecular C–O and C–C crosscoupling reaction of 1-hydroxy-7-methylcarbazole,[20] iron-mediated oxidative cyclization,[21] reaction of 2-cinnamoyl-1-hydroxycarbazoles under hydrogen peroxide/sodium hydroxide[22] and palladium(II)-catalyzed carbazole construction followed by pyran ring annulation.[23-28]

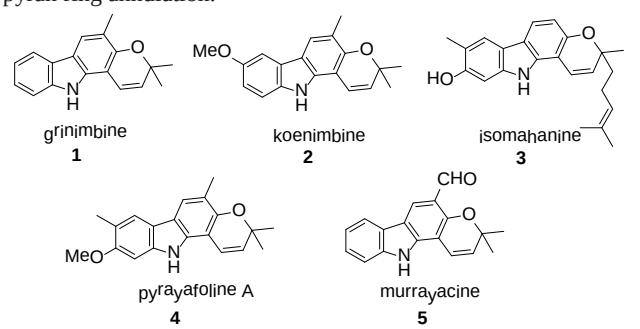

Fig. 1 Chemical Structures of pyran ring fused biologically active carbazoles.

[a]*Department of Chemistry, JNTUH college of Engineering, Kukatpally, Hyderabad (T.S), India-500 085. E-mail: padduiict@gmail.com*
[b]*CSIR – Indian Institute of Chemical Technology, Hyderabad, India–500 007, Phone: (+) 91-40-27192568*
[c]*Department of Chemistry, Gitam School of Technology, Gitam University, Hyderabad (T.S), India-502 102*

†Electronic Supplementary Information (ESI) available: ^{1}H NMR and ^{13}C NMR spectra of compounds are provided. See DOI: 10.1039/b000000x/

Recently Rajendra Prasad et al. reported the synthesis of pyrano[2,3-*a*]carbazoles from 1-hydroxycarbazole in the presence of $NaHCO_3$ by grinding at room temperature.[29] Herein, we have described the synthesis of new 2-amino-4,7-dihydro-4-phenylpyrano[3,2-*c*]carbazole-3-carbonitrile derivatives from 4-hydroxycarbazole *via* a simple and efficient one-pot reaction.

Results & Discussion

Chemistry

The synthesis of the target compounds (**9a–p**) was carried out as outlined in Scheme 1. Initially the reaction was carried out by treating equimolar amounts of 4-hydroxycarbazole, benzaldehyde and malononitrile with 1.0 equiv of triethylamine in ethanol at room temperature affording the 2-amino-4,7-dihydro-4-phenylpyrano[3,2-*c*]carbazole-3-carbonitirle in 85% yield. The scope and the generality of the present method were then further demonstrated by reaction of various aldehydes with malononitrile and 4-hydroxycarbazole (Table 1). Aromatic aldehydes bearing either electron-donating or electron-withdrawing substituents all worked well, giving good yields.

Further, the scope of this reaction was extended to ethylcyanoacetate instead of malononitrile. In this connection, 4-hydroxycarbazoles were treated with ethylcyanoacetate and various aldehydes in the presence of TEA and the expected products were obtained (Scheme 1). All synthesized compounds were characterized by NMR analysis and mass spectrometry. It was observed that cyclization was not achieved by using 2-hydroxycarbazole under similar reaction. To determine the efficiency of this procedure, reactions with various other bases such as piperidine, $NaHCO_3$, Na_2CO_3, K_2CO_3 was performed. Among them, TEA was found to be the most effective catalyst for this conversion.

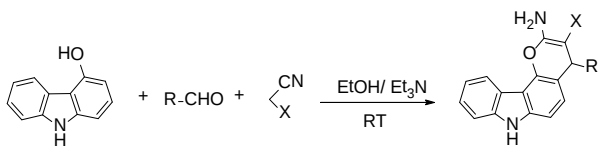

Scheme 1

Table 1. Pyrano[3,2-*c*]carbazole derivatives **9a-p** produced via Scheme 1

Compound	R	X	**9a-p**	Time (min)	Yield (%)
9a	3-$NO_2C_6H_4$	CN	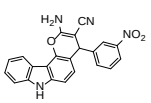	40	89
9b	4-$NO_2C_6H_4$	CN	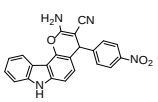	40	90
9c	4-CNC_6H_4	CN	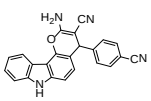	45	88
9d	4-F C_6H_4	CN	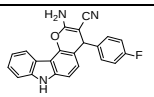	55	90
9e	4-Cl C_6H_4	CN	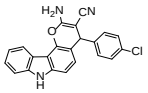	60	85
9f	4-Br C_6H_4	CN	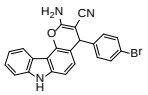	50	87
9g	C_6H_5	CN	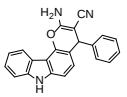	60	85
9h	4-$CH_3C_6H_4$	CN	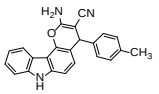	60	82
9i	3-OCH_3 C_6H_4	CN	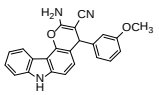	60	85
9j	2-pyridyl	CN	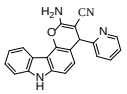	60	80
9k	3-pyridyl	CN	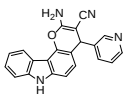	60	82
9l	4-NO_2 C_6H_4	COOEt	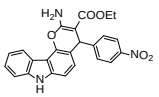	45	88
9m	4-CN C_6H_4	COOEt	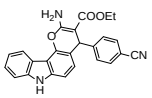	50	86
9n	4-Cl C_6H_4	COOEt	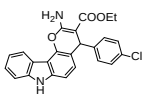	45	85
9o	4-Br C_6H_4	COOEt	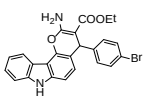	50	85
9p	C_6H_5	COOEt	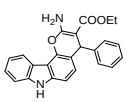	50	86

Biology

Antiproliferative activity

All the pyranocarbazole derivatives (**9a-p**) were assessed for their antiproliferative activity against a panel of four human cancer cell lines such as MDA-MB231 (breast carcinoma), K562 (chronic myeloid leukemia), A549 (lung cancer), HeLa (cervical cancer) and L929 (mouse connective tissue fibroblast cells) employing MTT assay. CombretastatinA-4 (CA-4) was taken as positive control. The congeners comprised of 5 rings (A, B, C, D and E) with different functionalization on D and E rings. Particularly the D and E rings were modified with substituent's like $–NO_2$, -CN, -F, -Cl, -Br, $-CH_3$, $-OCH_3$, $-COOC_2H_5$ while A, B and C rings were unchanged. Whereas, $–NH_2$ group present only on the D-

ring of the all compounds as unmodified. Based on the structure and activity relationship the congener's **9a-k** with C2-NH_2 and C3-CN groups on the D-ring exhibited potential cytotoxicity over the congeners **9l-p** that possess C2-NH_2 and C3-$COOC_2H_5$ on the same D-ring. Moreover, position and substitution change on the E-ring also showed a dramatic role in the potency of the pyranocarbazoles. In detail, the C-3 substituted compounds exhibited appreciable growth inhibitory effect, than the C-4 substituted compounds on the E-ring. Among all the congeners the compounds **9a, 9c, 9g, 9i** and **9m** showed profound antiproliferative activity on all the cancer cells with an IC_{50} value range 0.43-8.05 µM (Table 2). Interestingly, the representative compound **9i** with C-3 methoxy group on E-ring exhibited excellent activity in breast cancer MDA-MB 231 cells with IC_{50} value 0.43 µM. In comparison, the same compound manifested IC_{50} values of 1.1 µM and 3.4 µM in K562 and A549 cells respectively. Moreover, the compound **9i** showed a significant growth inhibition with IC_{50} values of 3.41 µM and 8.05 µM in A549 and Hela cells respectively. Compound **9a** bearing C-3 nitro on the E-ring also inhibited the growth of breast cancer and leukemia cancer cells with IC_{50} values of 0.55 µM in MDA-MB-231, 1.89 µM in K562. In comparison, compound **9g,** that is devoid of substitution on E ring inhibited cell growth with IC_{50} values of 1.26 µM in MDA-MB-231 and 2.78 µM in K562 cell line. In addition, all the compounds were shown slightest inhibitory effect against a noncancerous L929 cell line with the IC_{50} values near and above 100 µM, indicating these compounds have minimal or nontoxic towards the normal cells. To further elucidate the structure-activity relationships, E-ring was extensively modified with C-2 pyridine in compound **9j** and C-3 pyridine in compound **9k**. The resultant derivatives showed reduced cytotoxicity in all the tested cell lines. Furthermore, the congeners **9d, 9e, 9n** and **9o** with halogen atoms on the E-ring showed deleterious effects on the cell growth. Thus the overall cytotoxicity results suggested that the derivatives with electropositive (-OCH_3, -CH_3) and electronegative (-NO_2, -CN) substitutions demonstrated significant growth inhibitory effects compared to halogen substituted congeners. This could be attributed to the presence of huge electron densities around the halogen substituents on the E-ring. However, this statement is exempted in the case of **9g** due to devoid of halogen groups such as Cl, F and Br substituents on the E-ring.

Table 2. Antiproliferative activity of Pyrano[3,2-*c*]carbazole derivatives **9a-p** on various cancerous cell lines.

Compd	MDA-MB 231(µM) ±SD	K562 (µM) ±SD	A549 (µM) ±SD	HeLa (µM) ±SD	L929 (µM) ±SD
9a	0.55±0.2	2.02±0.1	6.87±1.2	8.05±0.7	88.14±1.3
9b	17.7±0.5	15.88±2.2	13.38±1.5	13.99±1.8	>100±6.8
9c	1.83±0.5	3.59±0.01	10.66±1.5	10.88±0.5	96±5.1
9d	14.04±1.5	8.89±0.4	13.06±1.7	19.90±2.1	>100±2.7
9e	13.12±1.8	7.28±1.1	16.40±0.2	18.71±0.2	>100±8.2
9f	19.6±0.6	14.70±0.6	12.06±0.8	21.62±1.7	>100±1.5
9g	1.26±0.5	3.10±0.1	1.13±0.04	9.82±0.2	>100±3.8
9h	16.4±1.5	16.26±3.7	11.41±2.6	14.02±1.6	>100±7.6
9i	0.43±0.3	1.13±0.1	3.41±0.07	6.12±0.4	69.24±3.4
9j	18.84±5.2	17.43±1.3	12.16±0.6	18.14±1.2	>100±1.9
9k	19.07±0.5	13.87±2.6	18.13±0.9	17.27±2.8	>100±5.3
9l	11.47±7.9	15.99±0.8	19.29±5.4	20.89±3.4	>100±4.8
9m	9.27±0.1	5.08±0.0	12.04±1.8	15.72±1.1	>100±8.7
9n	14.52±0.4	18.03±1.0	18.74±6.4	16.91±4.1	>100±5.9
9o	12.96±0.4	4.11±0.2	22.53±4.5	17.46±7.2	>100±4.5
9p	21.07±0.5	18.34±0.1	18.17±0.5	16.96±4.4	>100±7.2

Cell lines were treated with different concentrations of compounds. Cell viability was measured employing MTT assay. Concentration required to inhibition 50% cell growth and the values represent mean ± S.D. from three different experiments performed in triplicates.

Effect of 9a, 9c, 9g and 9i on cell cycle distribution

The pyranocarbazole derivatives that demonstrated significant antiproliferative activities were further analyzed for their affect on cell cycle. MDA-MB-231 cells were treated separately with compounds **9a**, **9c**, **9g** and **9i** at 1 µM concentrations for 24 h. CA-4 was used as positive control. Flow cytometry analysis revealed that compound treated cells accumulated at the G2/M phase of cell cycle with **9a** (82.95%), **9c** (80.30%), **9g** (46.27%) and **9i** (82.81%) arrest. In comparison, the DMSO treated cells showed normal distribution with more cell population in G1 phase. In contrast, cells treated with CA4 at 1 µM showed 57.79% of cell cycle arrest at G2/M phase. These results suggest that the pyranocarbazole derivatives inhibit cell growth due to arrest at G2/M phase of cell cycle.

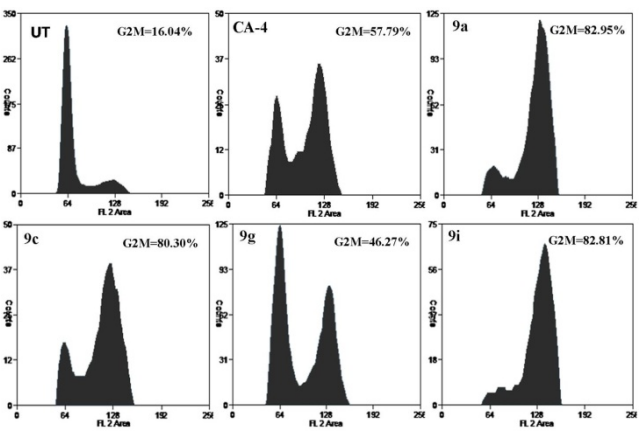

Fig. 2 FACS studies showing the induction of G2/M cell cycle arrest by compounds **CA-4, 9a**, **9c, 9g** and **9i** in MDA-MB-231 cells. Cells treated with each of the compounds at 1 µM concentration for 24 h were collected for the analysis. Untreated cells were analysed as control.

Effect of 9a, 9c, 9g and 9i on cellular cyclin-B1 levels by immunoblot analysis

To further confirm G2/M cell cycle arrest and to see the effect of

the same compounds at the protein level, we performed western blot analysis after isolating proteins from the treated and untreated cells. Cyclins are a group of proteins that are responsible for the control of cell cycle progression. Cyclin-B1 protein is a well characterized regulatory protein that plays a role in controlling mitosis. Accumulation of this protein is an indication of G2/M cell cycle arrest.[30,31] MDA-MB-231 cells were treated separately with compounds **9a, 9c, 9g** and **9i** at 1µM concentrations for 24 h. Total protein was isolated and western blot analysis was performed using anti cyclin-B1 antibody. Compound CA-4 was employed as positive control. Here the same blot was hybridized using anti b-Actin antibody that served as gel loading control to see the difference in the protein loading in each lane. Interestingly, compounds **9a** and **9i** that showed significant G2/M cell arrest expressed a highly induced level of cyclin-B1 compared to the CA-4 treated cells. However, **9c** and **9g** exhibited negligible effect on the cyclin-B1 protein expression when compared to untreated cells. Therefore, the accumulation of cyclin-B1 levels support that conjugates of Pyrano[3,2-*c*]carbazolesdemonstrate anticancer effects through G2/M cell cycle arrest.

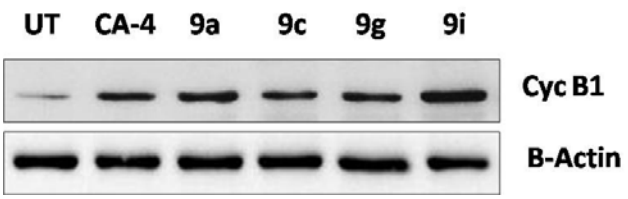

Fig. 3 Western blot analysis of Cyclin-B1: Proteins isolatedfromMDA-MB-231 cells treatedwith 1 µM concentrations of **9a, 9c, 9g** and **9i** for 24 h and subjected to western blotanalysis. Cells treated with compounds **9a** and **9i** produced significant elevation of cyclin B1 levels. b-Actin was employed as loading control. CA-4 was used as positive control and untreated as negetive control.

Effect of 9a, 9c, 9g and 9i on *invitro* tubulin polymerization

Many known antimitotic agents such as nocodazole, CA-4 and paclitaxel have been proven to show arrest at G2/M phase of cell cycle.[32] In the present study, pyranocarbazole derivatives induce a G2/M arrest. As G2/M arrest in many cases are due to defect in tubulin polymerisation, we wanted to see the effect of these compounds on tubulin polymerasation. Compounds **9a, 9c, 9g** and **9i** at 1 µM concentrations were incubated with tubulin for 30 min followed by tubulin polymerization assays (BK011, Cytoskeleton, Inc.) according to manufacturer's protocol. Interestingly, all the derivatives strongly inhibited tubulin polymerization and **9i** demonstrated 80% inhibition**.** Thus our results support that these pyranocarbazole derivatives indeed function as tubulin polymerization inhibitors and manifest their cytotoxicity.

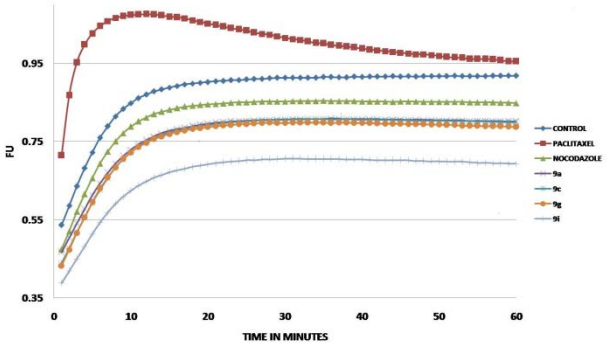

Fig. 4 Tubulin polymerization using the fluorescence based tubulin polymerization assay (BK011). Tubulin was incubated alone (Control), with Paclitaxel or Nocodazole and **9a, 9c, 9g** and **9i** at 1 µM concentration. Each condition was tested in triplicates. Polymerization was measured by excitation at 360 nm and emission at 420 nm for 60 min at 1min interwell. The average values were plotted, time on x-axis vs. fluorescence on y-axis.

Effect of 9a, 9c, 9g and 9i on microtubule network

Cancer cells challenged with tubulin inhibitors demonstrate G2/M arrest.[33] Typically large population of cells are stalled at metaphase of mitosis. Since the pyranocarbazole derivatives inhibit tubulin polymerization, we investigated their ability to disrupt microtubule network in MDA-MB-231 cells. Consequently, cells were grown on cover slips, followed by treatment with derivatives for 24 h at 1 µM concentrations and subjected to immunofluorescent studies using anti tubulin antibody. As expected, the compound treated cells, stained with tubulin antibody showed disrupted microtubule network. In contrast, the untreated cells contained fibrous microtubules.

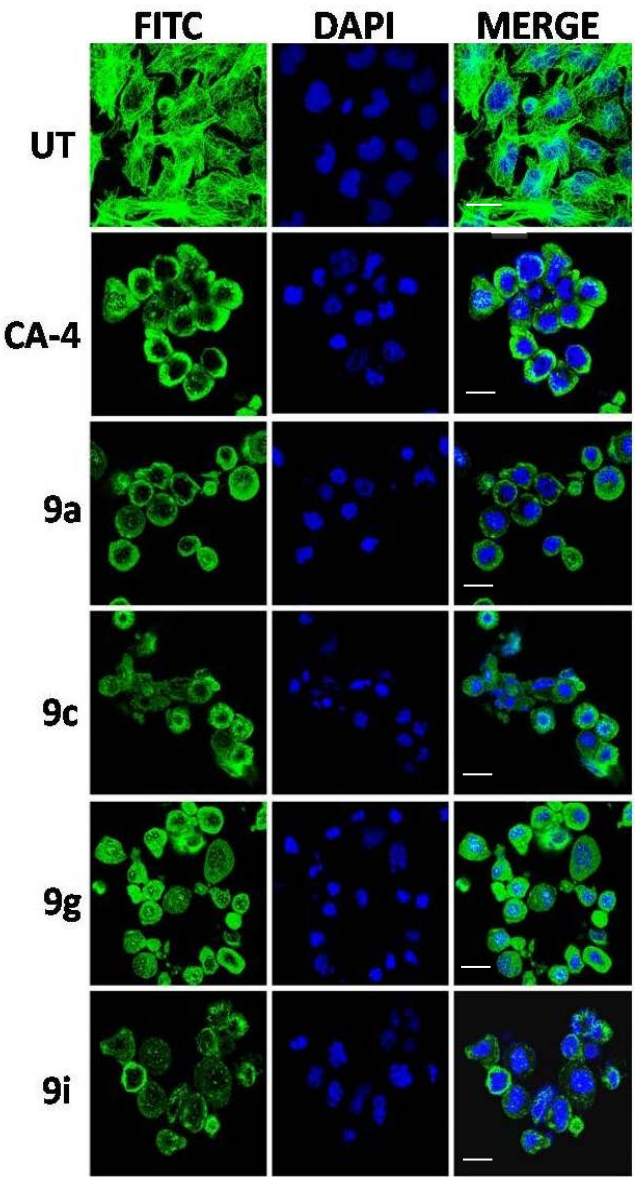

Fig. 5 Effect of **CA-4, 9a**, **9c, 9g** and **9i** on microtubules and nuclear condensation. MDA-MB-231 Cells were independently treated with **CA-4, 9a**, **9c, 9g** and **9i** at 1 µM concentration for 24 h. Following treatment, cells were fixed and stained for tubulin and FITC was used as secondary antibody. The cells were counterstained with DAPI. Slides were visualized under Olympus confocal fluorescence microscope equipped with FITC and DAPI filter settings using 60X objective. Photographs were take with FLOW VIEW FV 1000 series and analyzed with FV10ASW 1.7 series software. Cells stained for tubulin and DAPI from the same field of views are represented. Bar represents 20µM field length.

Effect of 9a, 9c, 9g and 9i on cellular tubulin polymerization

Since pyranocarbazole derivatives demonstrated potent inhibition of tubulin assembly, we analysed their effect on endogenous tubulin polymerization. MDA-MB-231 cells were treated with **9a, 9c, 9g** and **9i** at 1 µM concentrations for 24 h. Paclitaxel a tubulin polymerizing agent and CA-4, a tubulin depolymerising molecule was employed as positive controls. Untreated cells were utilized for control treatments. After 24 h of treatments, soluble fraction containing free tubulin and insoluble fraction of polymerized tubulin were harvested and subjected to immunoblot analysis. Interestingly, compound **9i** that demonstrated potent inhibition of *invitro* tubulin assembly, contained tubulin in the soluble fraction similar to CA-4. Untreated cells exhibited fairly equal amounts of tubulin in fractions, typically demonstrating the dynamic equilibrium between free and polymerized tubulin. Taken together, these results corroborated with arrest of cells at G2/M, disruption of microtubules and invitro inhibition of tubulin polymerization.

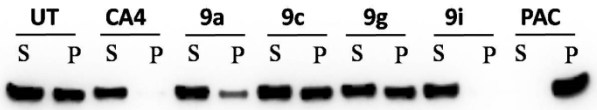

Fig. 6 Distribution of tubulin in soluble versus polymerized fractions as analyzed by immunoblotting

MDA-MB-231 cells were treated with **9a, 9c, 9g** and **9i** at the concentration of 1 µM for 24 h. The fractions containing soluble (S) and polymerized (P) tubulin were collected and separated by SDS-PAGE. Tubulin levels were detected by immunoblot analysis as described in the experimental section. Cells treated with CA-4 and paclitaxel (PAC) at 1 µM serves as positive and negative controls, whereas untreated cells shows the dynamic distribution of the soluble and polymerized fractions under similar experimental conditions.

Effect on caspase-3activation

Caspase-3 is one of the important proteins of cysteine-aspartic acid protease family that play a curtail role in cellular apoptosis and is usually associated with nuclear damage, cell shrinkage and fragmentation of cellular DNA. It is well reported that molecules that inhibit microtubule polymerization and cause mitotic arrest eventually lead to apoptosis.[34,35] Therefore, the effect of these compounds on the caspase-3 induction and successful programmed cell death in MDA-MB-231 cells was investigated. Cells were treated with **9a, 9c, 9g** and **9i** at 1 µM concentrations for 24 h and examined for caspase-3 activity. CA-4 treated cells were taken as reference standard compound, similar to above mentioned experiments. Compounds **9a** and **9i** which showed potent antimitotic effect also activated the caspase-3 compared to CA-4. Compounds **9c** and **9g** also showed a significant effect on caspase-3 but to a lesser extent than **9a** and **9i**. Hence, it may be concluded that the Pyrano[3,2-*c*]carbazole conjugates can cause caspase-3 induced apoptosis. The optimal order of these conjugates on caspase-3 activity was shown as **9i>9a>9c>9g**.

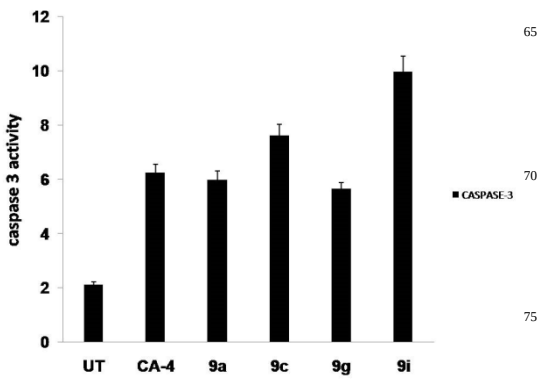

Fig. 7 Effect of compounds 9a, 9c, 9gand 9i on caspase-3 activity: MDA-MB-231 cells were treated with compounds **9a, 9c, 9g** and **9i** at 1 µM concentrations for 24 h. **CA-4** treated cells serve as positive control. The most potent compound **9i** activated the caspase-3 significantly fourfold to untreated and twofold when compared with CA4.

Molecular modelling

To rationalize the experimental results obtained, molecular docking studies were performed on representative compounds like **9a** and **9i** against tubulin structure. Autodock4 has been employed and the lead compounds docked in the colchicine binding pocket of tubulin (PDB code: 3E22).[36] It is well studied that the colchicine binding site is generally present at the interface of α, β-tubulin heterodimers.[37] The *α*- and *β*-subunits of tubulin have shown as pale green cartoon and the interacting amino acid residues are represented as thick green sticks. The lead compounds used for docking study were shown as yellow sticks and hydrogen bonds were denoted as black colored dots. In both the cases (**9a** and **9i**) A, B, C and D rings that are present as rigid structure majorly buried in beta subunit and the E-ring with substituted phenyl group placed at the interface of a and b subunits. Both compounds were surrounded with the amino acid residues like Asn100, Val182, Asn101, Ser178 and Thr179 (a-subunit), Lys254, Ala250, Asn249, Thr353, Tyr435, Met259, Cs241, Leu255 and Leu313. Specifically in the case of compound **9a** the NH of B-ring formed a strong hydrogen bond with O of Thr353 (NH---O, distance 1.9 A). The E-ring that possessing 3-nitrophenyl group showed number of important hydrophilic as well as hydrophobic interactions. Particularly the O of the nitro group showed strong hydrogen bonding interactions with NH of the Asn249 (O---HN, distance 2.8 A) and Ala 250 (O---HN, distance=3.0 A). In addition, this nitro group showed some hydrophobic interactions with Asn249 and Lys254 residues. However, some ionic interactions were also found between the nitro group and amino acid residues present in the b subunit. Whereas, the compound **9i** also exhibited some important hydrogen bonding interaction with the amino acid residues like Lys254 of b subunit and Thr179 of a subunit. Specifically NH of the B-ring formed a strong hydrogen bond with O of Lys254 (NH---O, distance=1.8 A) and the NH of the same Lys254 also showed hydrogen bonding with O of E-ring methoxy group (NH---O, distance=2.3 A). In addition, we observed the strong hydrogen bond between NH of the D-ring and O of Thr179 (NH---O, distance=2.0 A). Moreover, some hydrophobic interactions were noted between these compounds and surrounded amino acid residues. Therefore, these docking simulations suggested that the compound preferably occupy the colchicine binding site of tubulin. Probably this might be responsible for the inhibition of tubulin polymerization leading to apoptotic cell death.

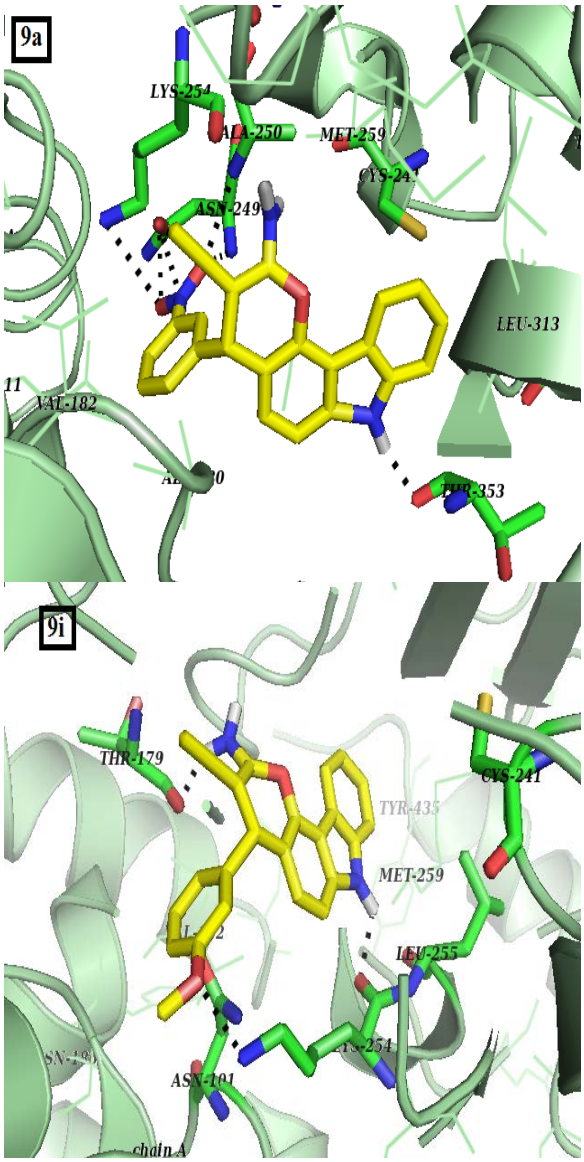

Fig. 8 Molecular docking poses of 9a and 9i at the colchicine binding site of tubulin. The a- b subunits were shown as pale green cartoon. The interacted amino acid residues of a and b subunits of tubulin were represented as green sticks where as the other amino acids were shown as green lines. The compounds were showed as yellow colored sticks. Both the compounds occupied the colchicines binding pocket of tubulin. The important hydrogen bonds formed between amino acid residues and compounds were denoted as black dots.

Conclusions

In conclusion, a library of new pyrano[3,2-*c*]carbazole derivatives (**9a-p**) were synthesized by a straightforward one-pot multicomponent synthesis, which involves simple isolation of the products by filtration and requires no further purification. Biological activity of these derivatives (**9a-9p**) revels that compounds **9a, 9c, 9g** and **9i** have potential cytotoxicity. Among the lead compounds **9a** and **9i** have shown significant anticancer activity by inhibiting tubulin polymerization that results G2/M

cell arrest and increased cyclinB1 cellular levels followed by increased caspase-3 activity that results apoptotic programmed cell death of the cancer cells.

Experimental Section

Chemistry

All chemicals were purchased from Lancaster (Alfa Aesar, Johnson Matthey Co, Ward Hill, MA, USA), Sigma-Aldrich (St Louis, MO, USA) and Spectrochem Pvt Ltd (Mumbai, India). Reactions were monitored by TLC, performed on silica gel glass plates containing 60 F-254 and visualization on TLC was achieved by UV light or iodine indicator. ^{1}H NMR spectra were recorded on Avance (300 MHz); Bruker, Fallanden, Switzerland instruments. Chemical shifts were reported in ppm, downfield from internal TMS standard. Spectral patterns were designated as s, singlet; d, doublet; dd, double doublet; t, triplet; td, triplet of doublet; bs, broad singlet; m, multiplet. ESI spectra were recorded on Micro mass, Quattro LC using ESI+ software with capillary voltage of 3.98 kV and ESI mode positive ion trap detector. IR spectra were recorded on a FT-IR spectrometer and only major peaks are reported in cm^{-1}.

General procedure for the preparation of compounds (9a-p)

A mixture of 4-hydroxy-9H-carbazole-3-carbaldehyde **6** (1 mmol), benzaldehyde **7** (1.2 mmol) and malononitrile/ethylcyano acetate **8** (1 mmol) were stirred in ethanol (5 ml) containing catalytic amount of Et_3N as a base at room temperature until completion of the reaction. After completion of the reaction, 15 ml of water was added to the reaction mixture and the separated solid was collected by filteration and dried to get **9**. Latter on recrystallization from suitable solvent to give pure compound **9**.

2-amino-4,7-dihydro-4-(3-nitrophenyl)pyrano[3,2-*c*]carbazole-3-carbonitrile (9a). MP: 252-254 ^{o}C; ^{1}H NMR (300 MHz, DMSO-d_6): δ 11.48 (s, 1H, –N*H*), 8.55 (d, 1H, *J* = 7.7 Hz, Ar–*H*), 8.20 (m, 2H, Ar–*H*), 7.60-7.30 (m, 6H, 4Ar–*H*, 2NH_2), 7.20 (m, 2H, Ar–*H*), 6.98 (d, 1H, *J* = 8.5 Hz, Ar–*H*), 5.12 (s, 1H, –C*H*–); ^{13}C NMR (75 MHz, DMSO-d_6): δ 160.5, 149.0, 147.9, 143.4, 140.0, 139.9, 139.6, 139.4, 134.4, 130.3, 126.0, 125.8, 125.6, 123.2, 121.8, 120.5, 120.2, 119.0, 111.1, 110.8, 110.0, 107.9; ESIMS: *m/z* 383 (M+H)$^+$; HRMS: *m/z* (M+H)$^+$ calcd for $C_{22}H_{15}O_3N_4$: 383.1204, found: 383.1211.

2-amino-4,7-dihydro-4-(4-nitrophenyl)pyrano[3,2-*c*]carbazole-3-carbonitrile (9b). MP: 262-264 ^{o}C; ^{1}H NMR (300 MHz, DMSO-d_6): δ 11.45 (s, 1H, –N*H*), 8.74 (d, 1H, *J* = 7.1 Hz, Ar–*H*), 8.61-8.45 (m, 2H, Ar–*H*), 8.25-8.04 (m, 3H, Ar–*H*), 8.00-7.90 (m, 1H, Ar–*H*), 7.83-7.61 (m, 3H, 1Ar–*H*, 2NH_2), 7.56-7.42 (m, 2H, Ar–*H*), 5.36 (s, 1H, –C*H*–); ^{13}C NMR (75 MHz, DMSO-d_6): δ 160.3, 154.1, 146.2, 143.4, 140.0, 139.5, 128.7, 126.0, 125.6, 123.9, 123.2, 120.3, 120.2, 119.0, 112.1, 110.8, 110.0, 109.8, 107.8, 55.4; ESIMS: *m/z* 383 (M+H)$^+$; HRMS: *m/z* (M+H)$^+$ calcd for $C_{22}H_{15}O_3N_4$: 383.1235, found: 383.1242.

2-amino-4-(4-cyanophenyl)-4,7-dihydropyrano[3,2-*c*]carbazole-3-carbonitrile (9c). MP: 220-222 ^{o}C; ^{1}H NMR (300 MHz, DMSO-d_6): δ 11.49 (s, 1H, –N*H*), 8.58 (d, 1H, *J* = 8.3 Hz, Ar–*H*), 7.53 (d, 1H, *J* = 7.8 Hz, Ar–*H*), 7.45 (t, 1H, *J* = 8.5 Hz, Ar–*H*), 7.37-7.13 (m, 8H, 6Ar–*H*, 2NH_2), 7.00 (d, 1H, *J* = 8.3 Hz, Ar–*H*), 4.96 (s, 1H, –C*H*–); ^{13}C NMR (75 MHz, DMSO-d_6): δ 160.1, 143.3, 143.0, 139.8, 139.5, 129.4, 129.2, 126.1, 125.4, 123.1, 120.6, 120.3, 118.9, 115.3, 115.0, 112.0, 110.7, 109.9, 107.6, 56.4; IR (KBr pellet, cm^{-1}): 3504, 3468, 3431, 3410, 2198, 1657, 1501, 1453, 1340, 1099; ESIMS: *m/z* 363 (M+H)$^+$; HRMS: *m/z* (M+H)$^+$ calcd for $C_{23}H_{15}ON_4$: 363.1779, found: 363.1787.

2-amino-4-(4-fluorophenyl)-4,7-dihydropyrano[3,2-*c*]carbazole-3-carbonitrile (9d). MP: 216-218 ^{o}C; ^{1}H NMR (300 MHz, DMSO-d_6): δ 10.89 (s, 1H, –N*H*), 8.46 (d, 1H, *J* = 7.1 Hz, Ar–*H*), 7.54-7.32 (m, 2H, Ar–*H*), 7.32-7.08 (m, 4H, Ar–*H*), 7.06-6.84 (m, 3H, 1Ar–*H*, 2NH_2), 6.50-6.32 (m, 2H, Ar–*H*), 4.87 (s, 1H, –C*H*–); ^{13}C NMR (75 MHz, DMSO-d_6): δ 160.1, 143.3, 143.0, 139.8, 139.5, 129.4, 129.3, 126.1, 125.5, 123.1, 120.6, 120.3, 118.9, 115.3, 115.1, 112.0, 110.7, 110.0, 107.6, 56.5; ESIMS: *m/z* 356 (M+H)$^+$; HRMS: *m/z* (M+H)$^+$ calcd for $C_{22}H_{15}ON_3F$: 356.1310, found: 356.1320.

2-amino-4-(4-chlorophenyl)-4,7-dihydropyrano[3,2-*c*]carbazole-3-carbonitrile (9e). MP: 248-250 ^{o}C; ^{1}H NMR (300 MHz, DMSO-d_6): δ 10.70 (s, 1H, –N*H*), 8.44 (d, 1H, *J* = 7.7 Hz, Ar–*H*), 7.57 (d, 1H, *J* = 5.1 Hz, Ar–*H*), 7.52-7.36 (m, 2H, Ar–*H*), 7.33-7.10 (m, 5H, 3Ar–*H*, 2NH_2), 6.90 (dd, 1H, *J* = 4.9, 8.1 Hz, Ar–*H*), 6.16 (m, 2H, Ar–*H*), 4.87 (s, 1H, –C*H*–); ^{13}C NMR (75 MHz, DMSO-d_6): δ 160.2, 145.7, 143.3, 139.8, 139.5, 131.1, 129.3, 128.5, 126.0, 125.8, 125.5, 123.1, 120.6, 120.2, 118.9, 111.7, 110.7, 109.9, 107.7, 56.2; ESIMS: *m/z* 372 (M+H)$^+$; HRMS: *m/z* (M+H)$^+$ calcd for $C_{22}H_{15}ON_3Cl$: 372.1572, found: 372.1570.

2-amino-4-(4-bromophenyl)-4,7-dihydropyrano[3,2-*c*]carbazole-3-carbonitrile (9f). MP: >270 ^{o}C; ^{1}H NMR (300 MHz, DMSO-d_6): δ 10.91 (s, 1H, –N*H*), 8.47 (d, 1H, *J* = 7.7 Hz, Ar–*H*), 7.53-7.34 (m, 4H, Ar–*H*), 7.26-7.10 (m, 4H, 2Ar–*H*, 2NH_2), 6.89 (d, 1H, *J* = 8.3 Hz, Ar–*H*), 6.47 (m, 2H, Ar–*H*), 4.85 (s, 1H, –C*H*–); ^{13}C NMR (75 MHz, DMSO-d_6): δ 160.2, 146.2, 143.3, 139.8, 139.5, 131.4, 129.7, 126.0, 125.5, 123.1, 120.6, 120.2, 120.0, 119.6, 118.9, 111.6, 110.8, 109.9, 107.7, 56.1; ESIMS: *m/z* 416 (M+H)$^+$; HRMS: *m/z* (M+H)$^+$ calcd for $C_{22}H_{15}ON_3Br$: 416.1466, found: 383.1477.

2-amino-4,7-dihydro-4-phenylpyrano[3,2-*c*]carbazole-3-carbonitrile (9g). MP: 244-246 ^{o}C; ^{1}H NMR (300 MHz, DMSO-d_6): δ 11.43 (s, 1H, –N*H*), 8.56 (d, 1H, *J* = 7.7 Hz, Ar–*H*), 7.49 (d, 1H, *J* = 8.1 Hz, Ar–*H*), 7.42 (t, 1H, *J* = 8.1 Hz, Ar–*H*), 7.35-7.28 (m, 2H, Ar–*H*), 7.28-7.16 (m, 7H, 5Ar–*H*, 2NH_2), 6.98 (d, 1H, *J* = 8.5 Hz, Ar–*H*), 4.87 (s, 1H, –C*H*–); ^{13}C NMR (75 MHz, DMSO-d_6): δ 160.2, 146.8, 143.3, 139.7, 139.5, 128.5, 127.4, 126.5, 126.3, 126.1, 125.4, 123.1, 120.7, 120.3, 118.9, 112.2, 110.7, 109.9, 107.5, 56.6; IR (KBr pellet, cm^{-1}): 3461, 3412, 3329, 2193, 1661, 1636, 1502, 1402, 1096, 750; ESIMS: *m/z* 338 (M+H)$^+$; HRMS: *m/z* (M+H)$^+$ calcd for $C_{22}H_{16}ON_3$: 338.1415, found: 338.1423.

2-amino-4,7-dihydro-4-p-tolylpyrano[3,2-*c*]carbazole-3-carbonitrile (9h). MP: 244-246 ^{o}C; ^{1}H NMR (300 MHz, DMSO-d_6): δ 11.43 (s, 1H, –N*H*), 8.53 (d, 1H, *J* = 7.7 Hz, Ar–*H*), 7.49 (d, 1H, *J* = 8.1 Hz, Ar–*H*), 7.41 (t, 1H, *J* = 8.1 Hz, Ar–*H*), 7.25-7.05 (m, 8H, 6Ar–*H*, 2NH_2), 6.95 (d, 1H, *J* = 8.5 Hz, Ar–*H*), 4.82 (s, 1H, –C*H*–), 2.25 (s, 3H, –CH_3); ^{13}C NMR (75 MHz, DMSO-d_6): δ 160.1, 143.8, 143.3, 139.7, 139.5, 135.6, 129.0, 127.4, 126.2, 125.4, 123.1, 120.8, 120.6, 120.3, 118.9, 112.4, 110.7,

109.9, 107.5, 56.7, 20.5; ESIMS: *m/z* 352 $(M+H)^+$; HRMS: *m/z* $(M+H)^+$ calcd for $C_{23}H_{18}ON_3$: 352.1223, found: 352.1228.

2-amino-4,7-dihydro-4-(3-methoxyphenyl)pyrano[3,2-*c*]carbazole-3-carbonitrile (9i). MP: 230-232 °C; ^{1}H NMR (300 MHz, DMSO-d_6): δ 10.66 (s, 1H, –N*H*), 8.43 (m, 1H, Ar–*H*), 7.62-7.33 (m, 3H, Ar–*H*), 7.28-7.09 (m, 3H, Ar–*H*), 7.01-6.68 (m, 3H, 1Ar–*H*, 2NH_2), 6.16-6.00 (m, 2H, Ar–*H*), 4.84 (s, 1H, –C*H*–), 3.82-3.70 (m, 3H, -OCH_3); ^{13}C NMR (75 MHz, DMSO-d_6): δ 160.3, 159.3, 148.4, 143.3, 139.8, 139.5, 129.6, 126.1, 125.4, 123.2, 120.7, 120.3, 119.7, 118.9, 113.6, 112.1, 111.4, 110.7, 109.9, 107.6, 56.5, 54.9, 30.6; ESIMS: *m/z* 368 $(M+H)^+$; HRMS: *m/z* $(M+H)^+$ calcd for $C_{23}H_{18}O_2N_3$: 368.1756, found: 368.1769.

2-amino-4,7-dihydro-4-(pyridin-3-yl)pyrano[3,2-*c*]carbazole-3-carbonitrile (9j). MP: >270 °C; ^{1}H NMR (300 MHz, DMSO-d_6): δ 11.48 (s, 1H, –N*H*), 8.58-8.52 (m, 2H, –C*H*–N–C*H*–), 8.44 (d, 1H, *J* = 4.7 Hz, Ar–*H*), 7.62-7.55 (m, 1H, Ar–*H*), 7.50 (d, 1H, *J* = 8.1 Hz, Ar–*H*), 7.42 (t, 1H, *J* = 7.9 Hz, Ar–*H*), 7.38-7.28 (m, 3H, 1Ar–*H*, 2NH_2), 7.25-7.16 (m, 2H, Ar–*H*), 6.98 (d, 1H, *J* = 8.5 Hz, Ar–*H*), 4.98 (s, 1H, –C*H*–); ^{13}C NMR (75 MHz, DMSO-d_6): δ 160.4, 148.6, 148.0, 143.5, 142.0, 139.9, 139.6, 135.2, 126.0, 125.6, 123.9, 123.2, 120.5, 120.3, 120.2, 119.0, 111.2, 110.8, 110.0, 107.8, 55.7; ESIMS: *m/z* 386 $(M+H)^+$; HRMS: *m/z* $(M+H)^+$ calcd for $C_{21}H_{15}ON_4$: 386.2988, found: 386.2984.

2-amino-4,7-dihydro-4-(pyridin-2-yl)pyrano[3,2-*c*]carbazole-3-carbonitrile (9k). MP: >270; ^{1}H NMR (300 MHz, DMSO-d_6): δ 11.43 (s, 1H, –N*H*), 8.53 (d, 1H, *J* = 7.7 Hz, –N–C*H*), 8.47 (d, 1H, *J* = 5.6 Hz, Ar–*H*), 7.75 (td, 1H, *J* = 7.7, 1.9 Hz, Ar–*H*), 7.49 (d, 1H, *J* = 8.1 Hz, Ar–*H*), 7.41 (td, 1H, *J* = 7.1, 1.1 Hz, Ar–*H*), 7.33 (d, 1H, *J* = 7.9 Hz, Ar–*H*), 7.27-7.14 (m, 5H, 3Ar–*H*, 2NH_2), 7.04 (d, 1H, *J* = 8.5 Hz, Ar–*H*), 4.98 (s, 1H, –C*H*–); ^{13}C NMR (75 MHz, DMSO-d_6): δ 164.4, 160.7, 149.2, 143.5, 139.9, 139.5, 137.0, 125.7, 125.6, 125.4, 123.1, 121.9, 121.6, 120.7, 120.3, 118.9, 111.3, 110.7, 110.0, 107.4, 55.0; ESIMS: *m/z* 386 $(M+H)^+$; HRMS: *m/z* $(M+H)^+$ calcd for $C_{21}H_{15}ON_4$: 386.1259, found: 386.1270.

Ethyl2-amino-4,7-dihydro-4-(4-nitrophenyl)pyrano[3,2-*c*]carbazole-3-carboxylate (9l). MP: >270 °C; ^{1}H NMR (300 MHz, DMSO-d_6): δ 11.45 (s, 1H, –N*H*), 8.60 (d, 1H, *J* = 7.7 Hz, Ar–*H*), 8.16-8.01 (m, 3H, Ar–*H*), 7.57-7.38 (m, 5H, 3Ar–*H*, 2NH_2), 7.27-7.14 (m, 3H, Ar–*H*), 5.21 (s, 1H, –C*H*–), 3.99 (q, 2H, *J* = 6.9 Hz, –OCH_2–CH$_3$), 1.08 (t, 3H, *J* = 7.1 Hz, –OCH$_2$–CH_3); ^{13}C NMR (75 MHz, DMSO-d_6): δ 168.1, 160.9, 156.7, 145.5, 143.4, 139.9, 139.5, 130.5, 128.4, 126.2, 125.5, 123.5, 123.1, 120.3, 118.9, 113.5, 110.8, 110.0, 107.6, 75.6, 58.7, 14.2; ESIMS: *m/z* 430 $(M+H)^+$; HRMS: *m/z* $(M+H)^+$ calcd for $C_{24}H_{20}O_5N_3$: 430.1043, found: 430.1045.

Ethyl 2-amino-4-(4-cyanophenyl)-4,7-dihydropyrano[3,2-*c*]carbazole-3-carboxylate (9m). MP: >270 °C; ^{1}H NMR (300 MHz, DMSO-d_6): δ 11.43 (s, 1H, –N*H*), 8.57 (d, 1H, *J* = 7.7 Hz, Ar–*H*), 8.05-7.98 (m, 2H, Ar–*H*), 7.68 (d, 2H, *J* = 8.1 Hz, Ar–*H*), 7.51-7.39 (m, 4H, 2Ar–*H*, 2NH_2), 7.24-7.12 (m, 3H, Ar–*H*), 5.13 (s, 1H, –C*H*–), 3.97 (q, 2H, *J* = 7.1 Hz, –OCH_2–CH$_3$), 1.06 (t, 3H, *J* = 7.1 Hz, –OCH$_2$–CH_3); ESIMS: *m/z* 410 $(M+H)^+$; HRMS: *m/z* $(M+H)^+$ calcd for $C_{25}H_{20}O_3N_3$: 410.1516, found: 410.1513.

Ethyl 2-amino-4-(4-chlorophenyl)-4,7-dihydropyrano[3,2-*c*]carbazole-3-carboxylate (9n). MP: 158-160 °C; ^{1}H NMR (300 MHz, DMSO-d_6): δ 10.63 (s, 1H, –N*H*), 8.50 (d, 1H, *J* = 7.7 Hz, Ar–*H*), 7.59 (m, 1H, Ar–*H*), 7.46 (d, 1H, *J* = 8.1 Hz, Ar–*H*), 7.43-7.35 (m, 2H, Ar-*H*), 7.27-7.10 (m, 6H, 4Ar–*H*, 2NH_2), 7.06-7.00 (m, 1H, Ar-*H*), 5.06 (s, 1H, –C*H*–), 4.07 (q, 2H, *J* = 7.1 Hz, -OCH_2-CH$_3$), 1.19 (t, 3H, *J* = 7.1 Hz, -OCH$_2$-CH_3); ^{13}C NMR (75 MHz, DMSO-d_6): δ 168.5, 160.9, 147.8, 143.3, 139.6, 139.4, 128.8, 128.6, 128.0, 127.9, 126.0, 125.3, 123.0, 120.2, 118.7, 114.8, 110.6, 110.0, 107.4, 76.0, 58.5, 14.1; ESIMS: *m/z* 419 $(M+H)^+$; HRMS: *m/z* $(M+H)^+$ calcd for $C_{24}H_{20}O_3N_2Cl$: 419.2381, found: 419.2375.

Ethyl 2-amino-4-(4-bromophenyl)-4,7-dihydropyrano[3,2-*c*]carbazole-3-carboxylate (9o). MP: 238-240 °C; ^{1}H NMR (300 MHz, DMSO-d_6): δ 11.41 (s, 1H, –N*H*), 8.58 (d, 1H, *J* = 7.7 Hz, Ar–*H*), 7.96 (m, 2H, Ar–*H*), 7.54-7.34 (m, 4H, 2Ar–*H*, 2NH_2), 7.30-7.07 (m, 5H, Ar–*H*), 5.03 (s, 1H, –C*H*–), 4.00 (q, 2H, *J* = 7.0 Hz, -OCH_2-CH$_3$), 1.10 (t, 3H, *J* = 7.0 Hz, -OCH$_2$-CH_3); ^{13}C NMR (75 MHz, DMSO-d_6): δ 168.2, 160.8, 148.5, 143.4, 139.6, 139.5, 131.3, 131.0, 129.3, 126.2, 125.4, 123.1, 120.3, 118.8, 118.5, 114.6, 110.7, 110.0, 107.4, 76.2, 58.5, 14.2; ESIMS: *m/z* 463 $(M+H)^+$; HRMS: *m/z* $(M+H)^+$ calcd for $C_{24}H_{20}O_3N_2Br$: 463.1753, found: 463.1745.

Ethyl 2-amino-4,7-dihydro-4-phenylpyrano[3,2-*c*]carbazole-3-carboxylate (9p). MP: 218-220 °C; ^{1}H NMR (300 MHz, DMSO-d_6): δ 11.39 (s, 1H, –N*H*), 8.57 (d, 1H, *J* = 7.7 Hz, Ar–*H*), 7.96-7.88 (m, 2H, Ar–*H*), 7.48 (d, 1H, *J* = 7.9 Hz, Ar–*H*), 7.41 (t, 1H, *J* = 7.9 Hz, Ar–*H*), 7.27-7.03 (m, 8H, 6Ar–*H*, 2NH_2), 5.02 (s, 1H, –C*H*–), 3.99 (q, 2H, *J* = 6.9 Hz, –OCH_2–CH$_3$), 1.08 (t, 3H, *J* = 6.9 Hz, –OCH$_2$–CH_3); ^{13}C NMR (75 MHz, DMSO-d_6): δ 168.4, 160.9, 149.0, 143.4, 139.6, 139.5, 128.0, 127.1, 126.2, 125.6, 125.3, 123.0, 120.3, 118.7, 115.3, 110.7, 109.9, 107.3, 76.7, 58.5, 14.2; IR (KBr pellet, cm^{-1}): 3435, 3315, 3293, 1671, 1485, 1221, 1091; ESIMS: *m/z* 385 $(M+H)^+$; HRMS: *m/z* $(M+H)^+$ calcd for $C_{24}H_{21}O_3N_2$: 385.1936, found: 385.1932.

Biology

Cell Cultures, maintenance and antiproliferative evaluation

All cell lines used in this study were purchased from the American Type Culture Collection (ATCC, United States). MDA-MB-231, A549, HeLa and L929 were grown in Dulbecco's modified Eagle's medium (containing 10% FBS in a humidified atmosphere of 5% CO_2 at 37 °C). K562 were grown in RPMI medium (containing 10% FBS in a humidified atmosphere of 5% CO_2 at 37 °C). Cells were trypsinized when sub-confluent from T25 flasks/60 mm dishes and seeded in 96-wel plates. The synthesized test compounds were evaluated for their *in vitro* antiproliferative in four different human cancer cell lines. A protocol of 24 h continuous drug exposure was used and a MTT cell proliferation assay was used to estimate cell viability or growth. Individual cell lines were grown in their respective media containing 10% fetal bovine serum and were seeded into 96-well microtiter plates in 200 µL aliquots at plating densities depending on the doubling time of individual cell lines. The microtiter plates were incubated at 37 °C, 5% CO_2, 95% air and 100% relative humidity for 24 h prior to addition of experimental drugs. Aliquots of 2 µL of the test compounds were added to the wells already containing 198 µL of cells, resulting in the required final drug concentrations. For each compound, five concentrations (0.01, 0.1, 1, 10 and 100 µM) were evaluated and each was done in triplicate wells. Plates were incubated further

for 24 h and the assay was terminated by the addition of 10 µL of 5% MTT and incubated for 60 min at 37 °C. Later, the plates were air-dried. Bound stain was subsequently eluted with 100 µL of DMSO and the absorbance was read in multimode plate reader (Varioscan Flash) at a wavelength of 560 nm. Percent growth was calculated on a plate by plate basis for test wells relative to control wells. The above determinations were repeated thrice. The growth inhibitory effects of the compounds were analyzed by generating dose response curves as a plot of the percentage surviving cells versus compound concentration. The sensitivity of the cancer cells to the test compound was expressed in terms of IC_{50}, a value defined as the concentration of compound that produced 50% reduction as compared to the control absorbance. IC_{50} values are indicated as means ± SD of three independent experiments.[38]

Analysis of cell cycle

MDA-MB-231 cells were grown in 60 mm dishes and were incubated for 24 h in the presence or absence of test compounds **9a, 9c, 9g** and **9i** at 1 μM concentration. Cells were harvested using Trypsin-EDTA, fixed with ice-cold 70% ethanol at 4 ^{o}C for 30 min, ethanol was removed by centrifugation and cells were stained with 1 mL of DNA staining solution [0.05 mg of Propidium Iodide (PI) and 100 μg RNase A] for 30 min in dark at 37 °C. The DNA contents of 20,000 events were measured by flow cytometer (BD MoFlo Legacy). Histograms were analyzed using Summit V4.3.[39]

Tubulin polymerization assay

An *in vitro* assay for monitoring the time dependent polymerization of tubulin to microtubules was performed employing a fluorescence based tubulin polymerization assay kit (BK011, Cytoskeleton, Inc.) according to the manufacturer's protocol. The reaction mixture in a final volume of 50 µl in PEM buffer (80 mM PIPES, 0.5 mM EGTA, 2 mM $MgCl_2$, pH 6.9) in 384 well plates contained 2 mg/mL bovine brain tubulin, 10 µM fluorescent reporter, 1 mM GTP in the presence or absence of test compounds at 37 ^{o}C. Tubulin polymerization was followed by monitoring the fluorescence enhancement due to the incorporation of a fluorescence reporter into microtubules as polymerization proceeds. Fluorescence emission at 420 nm (excitation wavelength is 360 nm) was measured for 1 h at 1 min intervals in a multimode plate reader (Tecan M200). To determine the IC_{50} values of the compounds against tubulin polymerization, the compounds were preincubated with tubulin at varying concentrations (0.01, 0.1, 1, 10 and 20 µM). Assays performed under similar conditions as employed for polymerization assays as described above.[38]

Immunohistochemistry of tubulin and analysis of nuclear morphology

MDA-MB-231 cells were seeded on glass cover slip, incubated for 24 h in the presence or absence of test compounds **9a, 9c, 9g, 9i** and **CA-4** at a concentration of 1 µM. Cells grown on coverslips were fixed in 3.5% formaldehyde in phosphate-buffered saline (PBS) pH 7.4 for 10 min at room temperature. Cells were permeablized for 6 min in PBS containing 0.5% Triton X-100 (Sigma) and 0.05% Tween-20 (Sigma). The permeablized cells were blocked with 2% BSA (Sigma) in PBS for 1 h. Later, the cells were incubated with primary antibody for tubulin from (sigma) at (1:200) diluted in blocking solution for 4 h at room temperature. Subsequently the antibodies were removed and the cells were washed thrice with PBS. Cells were then incubated with FITC labeled anti-mouse secondary antibody (1:500) for 1 h at room temperature. Cells were washed thrice with PBS and mounted in medium containing DAPI (vecta shield). Images were captured using the Olympus confocal microscope FLOW VIEW FV 1000 series and analyzed with FV10ASW 1.7 series software.

Western blot analysis of soluble versus polymerized tubulin

MDA-MB-231 cells were seeded in 12-well plates at 1×105 cells per well in complete growth medium. Following treatment of cells with respective compounds **9a, 9c, 9g** and **9i** for duration of 24 h, cells were washed with PBS and subsequently soluble and insoluble tubulin fractions were collected. To collect the soluble tubulin fractions, cells were permeablized with 200 µL of pre-warmed lysis buffer [80 mM Pipes-KOH (pH 6.8), 1 mM MgCl2, 1 mM EGTA, 0.2% Triton X-100, 10% glycerol, 0.1% protease inhibitor cocktail (Sigma-Aldrich)] and incubated for 3 min at 30 ^{o}C. Lysis buffer was gently removed and mixed with 100 µL of 3×Laemmli's sample buffer (180 mMTris-Cl pH 6.8, 6% SDS, 15% glycerol, 7.5% β-mercaptoethanol and 0.01% bromophenol blue). Samples were immediately heated to 95 ^{o}C for 3 min. To collect the insoluble tubulin fraction, 300 µL of 1×Laemmli's sample buffer was added to the remaining cells in each well and the samples were heated to 95 ^{o}C for 3 min. Equal volumes of samples were run on an SDS-10 % polyacrylamide gel and were transferred to a nitrocellulose membrane employing semidry transfer at 50 mA for 1 h. Blots were probed with mouse anti-human α-tubulin diluted 1:2000 µl (Sigma) and stained with rabbit anti-mouse secondary antibody coupled with horseradish peroxidase, diluted 1:5000 µl (Sigma). Bands were visualized using an enhanced Chemiluminescence protocol (Pierce) and radiographic film (Kodak).[40]

Caspase-3 Assay

MDA-MB-231 cells were seeded in 12 well plates as mentioned above and were treated with different compounds **9a, 9c** and **9i** at 1µM concentration. After 24 h of incubation with the compound, cells were lysed using lysis buffer and incubated at 4 ^{o}C for 10 min which then collected and spun at 4 ^{o}C, 10000 rpm for 10 min. The supernatant was collected which contains the protein. The protein was quantified employing Bradford Assay. Equal amount of protiens were added with assay buffer and caspase substrate which gives fluorescence units thereby calculated the activity against caspase.[41]

Molecular Modeling

AutoDock4 was employed to dock lead pyranocarbazole derivatives in colchicine binding site of tubulin.[42-43] Initial Cartesian coordinates for the protein-ligand complex structure were derived from crystal structure of tubulin (PDB ID: 3E22). The protein targets were prepared for molecular docking

simulation by removing water molecules, bound ligands. Hydrogen atoms and Kollman charges were added to each protein atom. Auto-Dock Tools-1.5.6 (ADT) was used to prepare and analyze the docking simulations for the AutoDock4. Coordinates of each compound were generated using Chemdraw 11.0 followed by MM2 energy minimization. The interaction of protein and ligands in binding pocket for Autodock4 was defined by a Grid box. The grid box was created with 60 points equally in each direction of x, y and z. AutoGrid4 was used to produce grid maps for AutoDock4 calculations where the search space size utilized grid points of 0.375 Å. The Lamarckian genetic algorithm was opted to search for the best conformers. Each docking experiment was performed 100 times, yielding 100 docked conformations. Parameters used for the docking were as follows: population size of 150; random starting position and conformation; maximal mutation of 2 Å in translation and 50 degrees in rotations; elitism of 1; mutation rate of 0.02 and crossover rate of 0.8 and local search rate of 0.06. Simulations were performed with a maximum of 1.5 million energy evaluations and a maximum of 50000 generations. Final docked conformations were clustered using a tolerance of 1.0 Å root mean square deviation. The best model was picked based on the best stabilization energy. Final figures for molecular modeling were visualized by using PyMol.[44]

Acknowledgements

P. Padmaja thanks Department of Science and Technology (DST) for INSPIRE Faculty Fellowship Award. K R G thanks UGC for his fellowship. MPB and NP thank CSIR 12th FYP CSC0111 (SMILE).

References

1. H. J. Knölker and K. R. Reddy, *Chem. Rev*., 2002, **102**, 4303.
2. A. Caruso, A. Chimento, H. El-Kashef, J. C. Lancelot, A. Panno, V. Pezzi, C. Saturnino, M. S. Sinicropi, R. Sirianni and S. J. Rault, *J. Enzym. Inhib. Med. Chem*., 2012, **27**, 609.
3. A. Caruso, A. S. Voisin-Chiret, J. C. Lancelot, M. S. Sinicropi, A. Garofalo and S. Rault, *Heterocycles*., 2007, **71**, 2203.
4. J. Sopkovà-de Oliveira Santos, A. Caruso, J. F. Lohier, J. C. Lancelot and S. Rault, *Acta Cryst*., 2008, **64**, 453.
5. J. F. Lohier, A. Caruso, J. Sopkovà-de Oliveira Santos, J. C. Lancelot and S. Rault, *Acta Cryst*., 2010, **66**, 1971.
6. A. W. Schmidt, K. R. Reddy and H. J. Knolker, *Chem. Rev*., 2012, **112**, 3193-3328.
7. A. Kuwabara, K. Nakano and K. Nozaki, *J. Org. Chem*., 2005, **70**, 413.
8. Z. Liu and R. C. Larock, *Tetrahedron*, 2007, **63**, 347.
9. A. Caruso, A. S. Voisin-Chiret, J. C. Lancelot, M. S. Sinicropi, A. Garofalo and S. Rault, *Molecule*, 2008, **13**, 1312.
10. T. A. Choi, R. Czerwonka, W. Frohner, M. P. Mrahl, K. R. Reddy, S. G. Franzblau and H. J. Knolker. *Chem. Med. Chem*., 2006, **1**, 812-815.
11. T. A. Choi, R. Czerwonka, R. Forke, A. Jager, J. Knoll, M. P. Krahl, T. Krause, K. R. Reddy, S. G. Franzblau and H. J. Knolker, *Med. Chem. Res*., 2008, **17**, 374-385.
12. H. J. Knölker, K. R. Reddy and G. A. Cordell (Eds.), *Academic Press: London*., 2008, **65**, 1-430.
13. R. S. Ramsewak, M. G. Nair, M. Strasburg, D. L. Dawitt and J. L. Nitiss, *J. Agri. Food Chem*., 1999, **47**, 444-447.
14. I. Master and J. Reisch, *Ann. Chem*., 1977, **10**, 1725.
15. S. Syam, A. B. Abdul, M. A. Sukari, S. Mohan, S. I. Abdelwahab and T. S. Wah, *Molecules*., 2011, **16**, 7155.
16. C. B. Cui, S. Y. Yan, B. Cai and X. S. Yao, *J. Asian Nat. Prod. Res*., 2002, **4**, 233.
17. Y. Tachibana, H. Kikuzaki, N. H. Lajis and N. Nakatani, *J. Agric. Food Chem*., 2003, **51**, 6461.
18. M. Itoigawa, Y. Kashiwada, C. Ito, H. Furukawa, Y. Tochibana, K. F. Bastow and K. H. Lee, *J. Nat. Prod*., 2000, **63**, 893.
19. P. R. Prasad and L. Yong Rok, *Synthesis*, 2012, **44**, 2910–2918.
20. K. Prabakaran, M. Zeller and K. J. R. Prasad, *Synlett*, 2011, **13**, 1835.
21. K. K. Gruner, T. Hopfmann, K. Matsumoto, A. Jager, T. Katsuki and H. J. Knolker, *J. Org. Biomol. Chem*., 2011, **9**, 2057.
22. M. Sridharan and K. J. R. Prasad, *Naturforsch*, 2008, **63**, 1112.
23. R. Hesee, K. K. Gruner, O. Kataeva, A. W. Schmidt and H. J. Knolker. *Chem. Eur. J*., 2013, **13**, 14098-14111.
24. V. P. Kumar, K. K. Gruner, O. Kataeva and H. J. Knolker. *Angew. Chem*., 2013, **52**, 11073-11077.
25. R. Hesse, A. Jager, A. W. Schmidt and H. J. Knolker, *Org. Biomol. Chem*., 2014, **12**, 3866-3876.
26. K. K. J. gruner, O. Kataeva, A. W. Schmidt and H. J. Knolker, *Chem. Eur. J*., 2014, **20**, 8536-8540.
27. R. Hesse, O. Kataeva, A. W. Schmidt and H. J. Knolker, *Chem. Eur. J*. 2014, **20**, 9504-9509
28. C. Gassner, R. Hesse, A. W. Schmidt and H. J. Knolker, *Org. Biool. Chem*., 2014, **12**, 6490-6499.
29. Y. Ezhumalai, P. Kumaresan, Z. Matthias and K. J. R. Prasad, *Synthetic Communications*., 2012, **42**, 1330–1340.
30. P. S. Frisa and J. W. Jacobberger, *PLoS One*., 2009, **4**, 7064.
31. A. Hwang, A. Maity, W. G. McKenna and R. J. Muschel, *J. Biol. Chem*., 1995, **270**, 28419-28424.
32. Y. S. Ho, J. S. Duh, J. H. Jeng, Y. J. Wang, Y. C. Liang, C. H. Lin, C. J. Tseng, C. F. Yu, R. J. Chen and J. K. Lin, *Int. J. Cancer*., 2001, **91**, 393-401.
33. H. I. Magalhaes, D. V. Wilke, D. P. Bezerra, B. C. Cavalcanti, R. Rotta, D. P. de Lima, A. Beatriz, M. O. Moraes, J. Diniz-Filho and C. Pessoa, *Toxicol Appl Pharmacol*., 2013, **272**, 117-26.
34. L. H. Zhang, L. Wu, H. K. Raymon, R. S. Chen, L. Corral, M. A. Shirley, R. K. Narla, J. Gamez, G. W. Muller, D. I. Stirling, B. J. Bartlett, P. H. Schafer and F. Payvandi, *Cancer Res*., 2006, **66**, 951-959.
35. T. M. Beale, D. M. Allwood, A. Bender, P. J. Bond, J. D. Brenton, D. S. Charnock-Jones, S. V. Ley, R. M. Myers, J. W. Shearman, J. Temple, J. Unger, C. A. Watts and J. Xian, *ACS. Med. Chem. Lett*., 2012, **19**, 3, 177-181.
36. S. Nitesh, J. Vaibhav, P. Ranjan, K. Somnath, D. Sarita, T. Neha, M. Purusottam, P. Garima, K. Maneesh, D. Dipon, R. Shakti, Satapathy, S. Sumit, K. Sankar, N. K. Guchhait, Chanakya and P. V. Bharatam, *Med. Chem. Commun*., 2014, **5**, 766-782.
37. R. Romagnoli, PG. Baraldi, A. Brancale, A. Ricci, E. Hamel, R. Bortolozzi, G. Basso, G. Viola. *J. Med. Chem*., 2011, **54**, 5144-5153.
38. A. Kamal, AB. Shaik, N. Jain, C. Kishore, A. Nagabhushana, B. Supriya, GB. Kumar, SS. Chourasiya, Y Suresh, RK. Mishra, A. Addlagatta 10.1016/j.ejmech.2013.10.077.
39. P. S. Frisa and J. W. Jacobberger, *PLoS One*., 2009, **4**, 7064.
40. A. S. Kumar, M. A. Reddy, N. Jain, C. Kishor, T. R. Murthy, D. Ramesh, B. Supriya, A. Addlagatta, S. V. Kalivendi and B. Sreedhar, *Eur. J. Med. Chem*., 2013, **60**, 305-324.
41. A. Kamal, F. Sultana, M. J. Ramaiah, Y. V. Srikanth, A. Viswanath, C. Kishor, P. Sharma, S. N. Pushpavalli, A.

Addlagatta, and M. Pal-Bhadra, *Chem. Med. Chem.*, 2012, **6**, 7, 292-300.

42. AutoDock,version4.0;http://www.scripps.edu/mb/olson/doc/autodock/.
43. M. A. Reddy, N. Jain, D. Yada, C. Kishore, J. R. Vangala, R. P. Surendra, A. Addlagatta, S. V. Kalivendi, B. Sreedhar, *J. Med. Chem.*, 2011, **54**, 6751.
44. W. L. DeLano, DeLano Scientific, San Carlos, CA, USA, http://www.pymol.org., 2002.